Environmental Science & Technology

pubs.acs.org/est

Article

Bottom-Heavy Trophic Pyramids Impair Methylmercury Biomagnification in the Marine Plankton Ecosystems

Peipei Wu, Stephanie Dutkiewicz, Erwan Monier, and Yanxu Zhang*

Cite This: https://doi.org/10.1021/acs.est.1c04083

Read Online

ACCESS | Metrics & More | Article Recommendations | Supporting Information

ABSTRACT: Methylmercury (CH_3Hg^+, MMHg) in the phytoplankton and zooplankton, which form the bottom of marine food webs, is a good predictor of MMHg in top predators, including humans. Therefore, evaluating the potential exposure of MMHg to higher trophic levels (TLs) requires a better understanding of relationships between MMHg biomagnification and plankton dynamics. In this study, a coupled ecological/physical model with 366 plankton types of different sizes, biogeochemical functions, and temperature tolerance is used to simulate the relationships between MMHg biomagnification and the ecosystem structure. The study shows that the MMHg biomagnification becomes more significant with increasing TLs. Trophic magnification factors (TMFs) in the lowest two TLs show the opposite spatial pattern to TMFs in higher TLs. The low TMFs are usually associated with a short food-chain length. The less bottom-heavy trophic pyramids in the oligotrophic oceans enhance the MMHg trophic transfer. The global average TMF is increased from 2.3 to 2.8 in the warmer future with a medium climate sensitivity of 2.5 °C. Our study suggests that if there are no mitigation measures for Hg emission, MMHg in the high-trophic-level plankton is increased more dramatically in the warming future, indicating greater MMHg exposure for top predators such as humans.

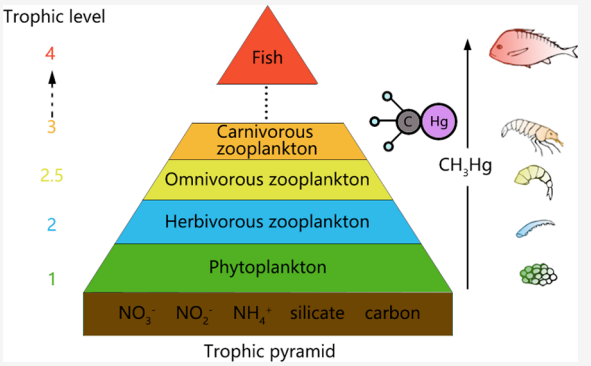

KEYWORDS: *prey, predator, trophic level, biomagnification*

1. INTRODUCTION

Methylmercury (CH_3Hg^+, MMHg) is a strong neurotoxin that can induce neurocognitive defects in fetuses and cardiovascular diseases in grown-ups.[1−3] Human's MMHg exposure is primarily from the ever-increasing consumption of seafood.[4−7] Once MMHg passes through cell membranes, it strongly binds with protein sulfhydryl or selenium and is very slow to be eliminated.[8] Therefore, MMHg undergoes significant biomagnification in the marine food webs. The MMHg level in seafood such as fish is largely controlled by MMHg in the lower trophic levels (TLs), especially the plankton that is at the base of marine food webs,[9,10] including its community composition and grazing relationships.[11]

Food webs are substantially different from oligotrophic to eutrophic oceans.[12−15] The biomass pyramids are more bottom-heavy in productive areas, while "inverted" pyramids can be found in oligotrophic areas.[12,14] In oligotrophic oceans, a relatively high proportion of predators consume more production, enhancing the energy transfer efficiency.[13,15] In contrast, zooplankton biomass saturates with increasing phytoplankton biomass, suggesting that grazing pressure is less intense in areas with dense populations.[16] Diversity, an important factor that affects the stability of ecosystems, peaks at intermediate levels of productivity, while massive blooms result in minimum diversity.[17] Global warming will change the primary production and reorganize the structure of ecosystems,[18,19] thereby altering the trophic transfer efficiency.[20,21]

Previous studies have found that the geographical variability in the structure and dietary habits of the ecosystems[22,23] can influence the accumulation of MMHg in the global marine food webs.[24−26] Lavoie et al.[26] found that trophic magnification slope in aquatic food webs was positively correlated with the latitude, and MMHg magnification was the most significant in cold and low-productivity regions. Higher productivities induce the "growth dilution" of MMHg,[27] leading to a lower efficiency of MMHg trophic transfer,[25,28] while MMHg biomagnification is more significant in oligotrophic oceans due to the slow growth rate.[29] Besides trophic states, food-chain length matters in the transfer of contaminants to top predators, and low mercury (Hg) biomagnification is associated with short food chains.[30]

Observational studies are usually conducted at a single site and are limited by sample sizes, which makes it hard to

Received: June 22, 2021
Revised: October 23, 2021
Accepted: October 25, 2021

compare across different ecosystems. Global models have been developed to simulate MMHg transfer in the marine organisms at low TLs, but the structure of plankton communities is highly simplified and only includes a handful of representative plankton function groups.[24,31] In this study, the MMHg model is coupled with an ecosystem model that incorporates 366 plankton types of different sizes, biogeochemical functions, and temperature tolerances.[32] We explore the relationships between the MMHg biomagnification and a variety of holistic indicators for plankton ecosystems, including the shape of trophic pyramids, primary production, and food-chain length. We also simulate the ecosystem dynamics in both present and future climate change scenarios.

2. METHODS

2.1. General Description. The marine plankton ecosystem and trophic transfer of MMHg are simulated in the MIT Integrated Global Systems Model (IGSM) framework.[32−34] This model framework simulates the physical and biogeochemical cycles of different plankton types and Hg species in the global ocean. Similar model frameworks have been applied in previous studies.[24,31,35] The model has a horizontal resolution of 2° × 2.5° with 22 vertical layers. The ocean circulation data are from the IGSM.[34] The simulation of the ocean boundary layer physics is based on Large et al.,[36] and the effects of mesoscale eddies are modeled according to Gent and McWilliams.[37] In this study, due to the high computational demand of the climate/ecosystem/MMHg modeling framework, we use a single climate simulation from an ensemble of perturbed initial conditions, perturbed physics (climate sensitivity), and varied emission scenarios.[38] The climate simulation is under a business-as-usual scenario that is similar to the Representative Concentration Pathway 8.5 (RCP8.5), with a medium climate sensitivity (2.5 °C).[39] We elaborate on the plankton ecosystem and the trophic transfer of MMHg below.

2.2. Ecosystem Model. The ocean plankton biogeochemistry and ecology are simulated by an ecosystem model that resolves diverse size classes, functional types, and thermal norms.[32] Detailed descriptions and parameter values are provided in that article. The model includes six functional groups: pico-phytoplankton, coccolithophores (that calcify), nitrogen-fixing cyanobacteria (diazotrophs), diatoms (that utilize silicic acid), mixotrophs (that photosynthesize and graze on other plankton), and zooplankton. The equivalent spherical diameter of the simulated plankton varies from 0.6 to 2425 μm with 4 size classes for the pico-phytoplankton (0.6−2 μm), 5 size classes for coccolithophores and diazotrophs (3−15 μm), 11 size classes for diatoms (3−155 μm), 10 size classes for mixotrophic dinoflagellates (7−228 μm), and 16 size classes for the zooplankton (6.6−2425 μm). For the phytoplankton and mixotrophic dinoflagellates, each size class is divided into 10 thermal norms, which set the temperature tolerance range over which the plankton can grow.

The zooplankton and mixotrophic dinoflagellates both graze on the plankton (phytoplankton or zooplankton) 5 to 20 times smaller than themselves, among which the 10 times smaller ones are the preferential choice (schematically shown in Figure S1 in size classes and functional types). However, the zooplankton have higher maximum grazing rates than mixotrophic dinoflagellates of the same size.[40] The palatability of predators to prey differs in functional groups. For instance, predators prefer the plankton with hard coverings less (e.g., coccolithophores and diatoms).

Sourcing from the death of all populations, the particulate and labile dissolved organic matters are explicitly modeled,[32] while an established data set of recalcitrant dissolved organic carbon (DOC) is used as an input into the model.[41] According to eq 1, the MMHg content in the phytoplankton is influenced by the total (labile and recalcitrant) DOC, while only the labile DOC affects through remineralization to the inorganic form.

The ecosystem model is numerically integrated forward in time under a present and a future scenario with high greenhouse gas emissions.[34,38] The seasonally varying quasi-steady plankton biomass, grazing fluxes, and mortality fluxes from the two scenarios are used as inputs for the MMHg model. The mortality fluxes represent all losses excluding grazing (e.g., cell death and viral lysis) for the plankton that have explicit predators in the model. A density-dependent term is used to parameterize the grazing by higher TLs for the zooplankton without explicitly modeled predators.

2.3. MMHg Model. The MMHg model is based on Wu et al. and Zhang et al.[24,31,35] The physical and biogeochemical cycles of the marine MMHg are simulated: air−sea exchange, river discharge, redox reactions, sinking of particle mercury, methylation, demethylation, and the trophic transfer of mercury in marine plankton food webs.

MMHg in seawater passively crosses the cell membrane (diffusion) and then accumulates in the phytoplankton:

$$\mathrm{MMHg_{phy}} = \mathrm{VCF}(d, [\mathrm{DOC}])\cdot \mathrm{MMHg_{sea}} \quad (1)$$

where $\mathrm{MMHg_{phy}}$ and $\mathrm{MMHg_{sea}}$ are the MMHg concentrations of the phytoplankton and seawater, respectively. The volume concentration factor is a function of the cell diameter d and total DOC concentrations (Table S1).[27] By affecting the rate of MMHg entering the phytoplankton cells, the distribution of DOC influences the spatial pattern of MMHg in the plankton.[24]

After entering the phytoplankton, MMHg is progressively transferred to higher TLs by the following processes: (1) MMHg intake directly from seawater; (2) MMHg absorption from the diet; (3) MMHg released after death; and (4) MMHg excretion:

$$\frac{\mathrm{dMMHg_{pred}}}{\mathrm{d}t} = k_{\mathrm{BC}}\cdot \mathrm{MMHg_{sea}} + k_{\mathrm{GR}}\cdot \mathrm{AE_{MMHg}}\cdot \mathrm{MMHg_{prey}} - (k_{\mathrm{MT}} + k_{\mathrm{EX}})\cdot \mathrm{MMHg_{pred}} \quad (2)$$

where $\mathrm{MMHg_{pred}}$ is the MMHg concentration in predators (i.e., zooplankton and mixotrophic dinoflagellates) and $\mathrm{MMHg_{prey}}$ is the MMHg concentration in prey (i.e., all plankton 5 to 20 times smaller than the predators). k_{BC}, k_{GR}, k_{MT}, k_{EX}, and $\mathrm{AE_{MMHg}}$ are the bioconcentration rate, grazing rate, mortality rate, excretion rate, and MMHg assimilation efficiency for the predators, respectively (Table S1).

The MMHg model is run from the year 2000 to 2015 in the "present" scenario and from 2085 to 2100 in the "future" scenario. In the above two experiments, we hold the atmospheric Hg concentration and deposition fluxes constant to diagnose the effect of a changing ocean ecosystem. The model's initial conditions for the two scenarios are from Zhang et al.,[31] and the concentration of atmospheric Hg and its deposition fluxes are from the output of the GEOS-Chem model.[42] Also, when the MMHg model is run from 2085 to

https://doi.org/10.1021/acs.est.1c04083
Environ. Sci. Technol. XXXX, XXX, XXX−XXX

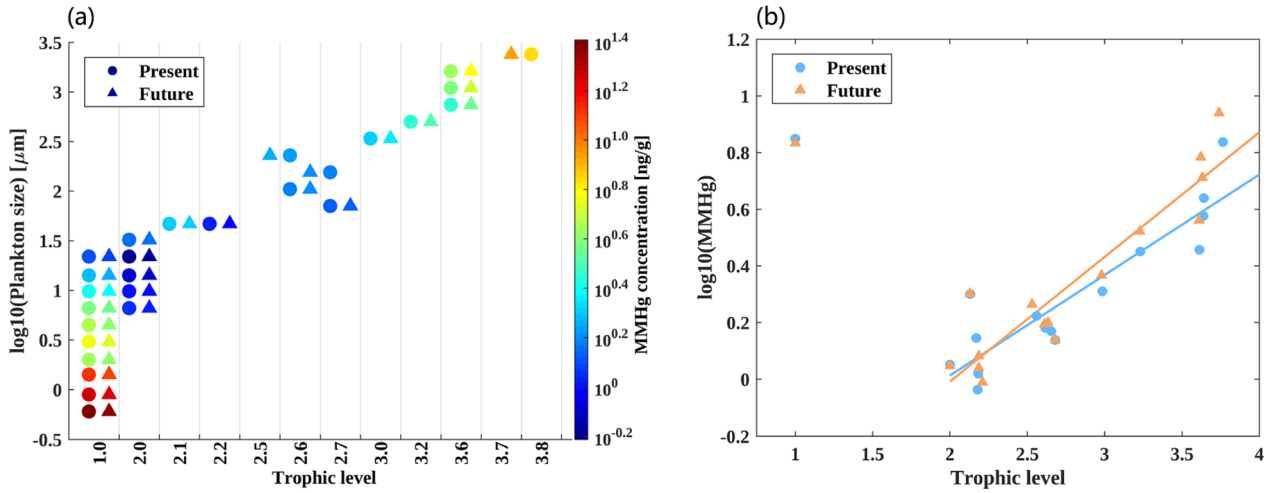

Figure 1. (a) Global average MMHg concentrations in the plankton of different body sizes and TLs. (b) Global average MMHg concentrations in the plankton at different TLs. The lines indicate the linear relationship between the base-10 logarithm of MMHg concentration and TL 2−4. The circle and triangle markers indicate the "present" and "future" experiment, respectively.

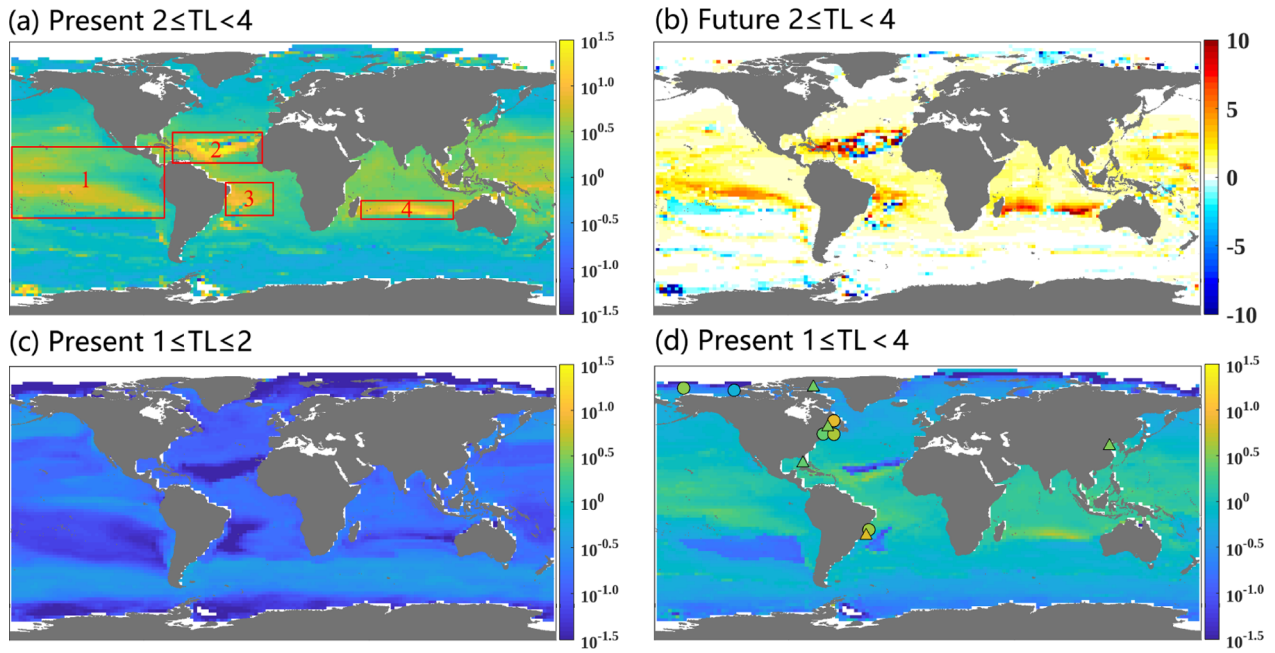

Figure 2. Modeled spatial pattern of TMFs in the global ocean: (a) TMFs between TLs 2 and 4 in the "present" experiment; (b) changes of TMFs in the "future"" experiment; (c) TMFs between TLs 1 and 2; and (d) TMFs between TLs 1 and 4. The red boxes superimposed on the maps show the regions with high TMFs: (1) the tropical Pacific Ocean except for the equatorial regions, (2) the South-Sargasso Sea, (3) the Brazilian Atlantic gyre, and (4) the South Indian gyre. Circles and triangles in (b) show the observed TMFs of MMHg[51−56] and total Hg[52,57−60] in marine plankton systems (for more details, see Table S2).

2100, we use the DOC, particle organic carbon, and chlorophyll from the ecosystem model with the present scenario. These variables affect the formation of MMHg.[31] The average of the last 5 years' results is used for analyses.

2.4. TL and Trophic Magnification Factor. The position of an organism in the food chain is defined as the TL. The TL of the phytoplankton (producer) is set as 1 and that of herbivorous zooplankton (primary customer) is set as 2. The TL of the omnivorous zooplankton and the carnivorous zooplankton is larger than 2 and is defined as[43]

$$TL_i = 1 + \sum_j (TL_j \cdot DC_{i,j}) \quad (3)$$

where TL_i is the TL of the predator i, TL_j is the TL of prey j of predator i, and $DC_{i,j}$ is the fraction of prey j in the diet of predator i.

The TL is assumed to be the primary driver of bioaccumulated contaminants in food webs as diet is the major route of exposure.[44] The relationship between the base-10 logarithm of MMHg concentration and the TLs is calculated as[26,44]

$$\log_{10}[\mathrm{MMHg}] = b\mathrm{TL} + a \quad (4)$$

where a is the intercept and b is the slope of the relationship, which varies with space and time. The trophic magnification factor (TMF) is defined as[44]

https://doi.org/10.1021/acs.est.1c04083
Environ. Sci. Technol. XXXX, XXX, XXX−XXX

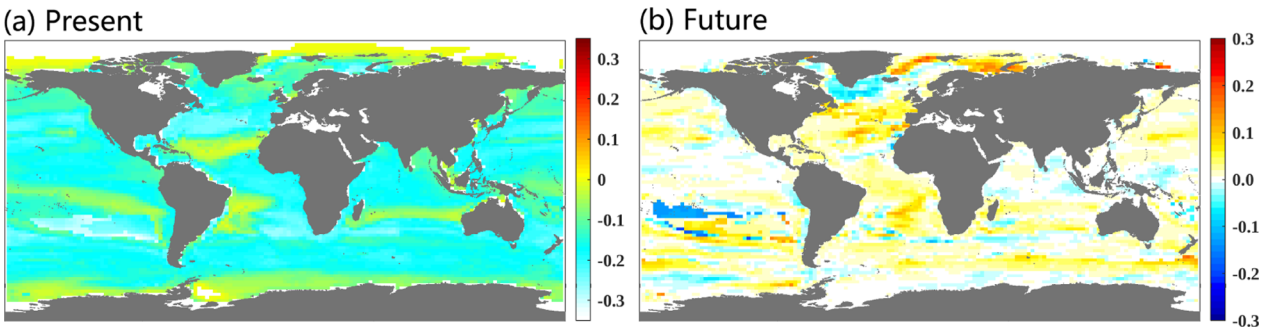

Figure 3. Modeled spatial pattern of the slopes between biomass and TLs 2–4 (TPS) in the global ocean: (a) TPS in the "present" experiment and (b) changes of TPS in the "future" experiment.

$$TMF = 10^{b} \quad (5)$$

3. RESULTS AND DISCUSSION

3.1. General MMHg Bioaccumulation and Biomagnification. Figure 1 shows the average MMHg concentrations in the plankton of different body sizes and TLs. The TLs of the modeled plankton range from 1 to 4, which are positively correlated with size because the predation and energy transfer are influenced by the body size.[32,45] The modeled ecosystem and MMHg in seawater have been evaluated against measured data in previous studies.[31,32] In this study, the MMHg concentrations are reported as wet weight. The modeled average MMHg concentration in the phytoplankton other than pico-phytoplankton is 3.4 ng/g, which is within the range of measured data in the central Pacific (0.1–4 ng/g).[46] The average MMHg concentration in the pico-phytoplankton is much higher (18.5 ng/g) due to their high cell surface area to volume ratios, which lead to high MMHg uptake efficiencies. Unfortunately, there are no measured data for such small size classes; however, high concentrations have been found in pure experimental pico-phytoplankton cultures.[47] In contrast to the phytoplankton, MMHg concentrations in large predators (mixotrophic dinoflagellates and zooplankton) are higher than in smaller ones due to significant biomagnification (Figure 1a). The modeled average MMHg concentrations in predators vary from 0.6 to 6.9 ng/g, consistent with the observed range (0.2–3.4 ng/g in the central Pacific[46] and 1.9–4.1 ng/g in the Southern Ocean[48]).

With the increase in the TL, the biomagnification of MMHg becomes more significant (Figures 1, 2, and S1). The global average TMF among all TLs (i.e., 1–4) is 1.3, while the TMF among consumers (i.e., 2–4) is 2.3 (Figure 1b). The mean modeled MMHg levels in TL 1 (phytoplankton) are higher than their predators. Overall, the TMFs between the lowest two TLs are less than 1, which indicates trophic dilution (Figure 2c). Indeed, the modeled phytoplankton community contains species with a wide range of sizes, and their MMHg concentrations also vary drastically even though they have the same TL (Figure 1a). The larger phytoplankton group seems to fit the regression between the TL and MMHg concentrations, whereas the smaller phytoplankton groups do not (Figure S1). This result is consistent with the previous findings with a simpler plankton community structure.[24,31] Compared with mixotrophic dinoflagellates, biomagnification is more significant between zooplankton and their prey due to higher grazing rates of the zooplankton (Figure S1). This indicates that MMHg biomagnification depends on the physiological characteristics of the plankton (e.g., sizes and grazing rates) and their TL positions in the food webs.

3.2. MMHg Biomagnification and Plankton Ecosystem Structure. Figure 2 shows the global spatial pattern of MMHg TMFs. The spatial pattern of TMFs is strongly correlated with the holistic characteristics of ecosystems (Figure 3). The trophic pyramids indicate the biomass distribution and energy flow in the ecosystems,[49] which affect the MMHg trophic transfer.[50] Here, we use the slope between biomass and the TLs to reflect the shape of the trophic pyramids (trophic pyramid's slope, TPS. TPSs at several selected grid points are shown in Figure S7). A threshold value of 10^{-5} mmol c m^{-3} is used to determine the presentence or absence of a plankton type in a given community.

High TMFs between TLs 2 and 4 are found in the South-Sargasso Sea, the Brazilian Atlantic gyre, the South Indian gyre, and the tropical Pacific Ocean except for the equatorial regions (Figure 2a), where the TPSs are also relatively high. TMFs between TLs 1 and 2 present the opposite spatial pattern to the TMFs between TLs 2 and 4 (Figure 2a,c). TMFs in the high-latitude ocean are relatively low, reflecting the relatively shorter food chains (Figure 4). In the Southern Ocean, where diatoms are dominant, high TLs (≥3) are absent (Figures S2 and 4).

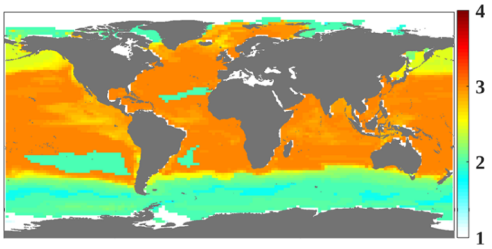

Figure 4. Modeled food-chain length in the global ocean.

Empirical studies for MMHg biomagnification in the global open ocean are rather limited. Large uncertainties thus exist for the model results, which are more reliable for the spatial patterns and trends instead of the absolute magnitudes. Overall, our modeled TMF among all TLs is close to the observation near the tropical estuarine Guanabara Bay (Figure 2d).[51] Modeled TMFs in the Atlantic and Arctic Ocean are lower than the empirical studies, but this is difficult to evaluate as there are inconsistencies in the definition of TLs and the differences in the units used (e.g., TLs determined by $\delta^{15}N$ vs diet, dry vs wet weight basis). However, we capture the trend

https://doi.org/10.1021/acs.est.1c04083
Environ. Sci. Technol. XXXX, XXX, XXX−XXX

that TMFs in the Atlantic Ocean are higher than those in the Arctic Ocean[52−56] (Figure 2d).

Figure 5 shows the relationships between TMFs and TPSs. We exclude the polar regions due to the much shorter food chain length (Figure 4). We find that in the low- and mid-latitude oceans, TMFs are positively correlated with the TPS. Relatively high TPSs are usually found in oligotrophic regions with low primary production and plankton biomass (Figures 3a and S3a), which is confirmed by a large number of ecological communities in nature.[12,14] Both previous and our studies simulated low zooplankton/phytoplankton ratios in oligotrophic waters (Figure S4).[61] This seems to be opposite to the spatial pattern of TPSs probably because the definition of TPS distinguishes the TLs. A field study across 58 lakes in the northeastern United States found that high plankton biomass reduces mercury biomagnification.[28] Also, a worldwide meta-analysis suggested that Hg biomagnification is highest in low-productivity systems.[26]

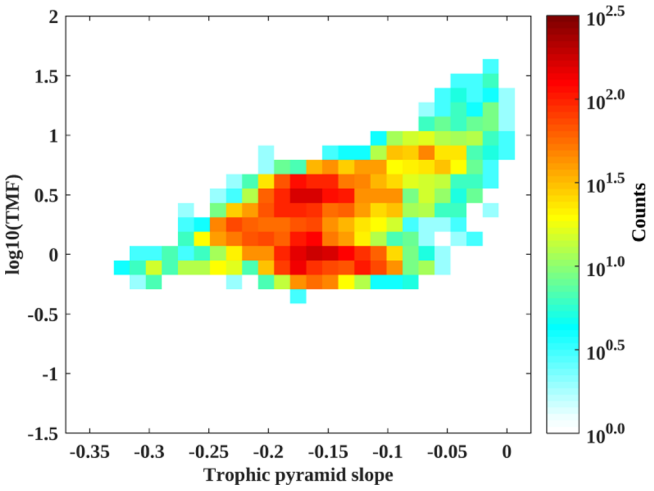

Figure 5. Relationships between TMFs and TPSs ($2 \leq TL < 4$) in the low- and mid-latitude oceans (−60−60°N). Colors represent the number of grid points.

In the oligotrophic waters, very tight and efficient coupling between the phytoplankton and heterotrophs enhances the capacity to support more predator biomass and the biomass is less dense-dependent, as indicated by previous studies,[12,14] which also explains the high TPSs as discussed above. More consumers and intense grazing pressure propagate more flows to high TLs. Diet is the primary source of MMHg[27] and higher grazing flux can greatly enhance the biomagnification.[24] Besides the less grazing flux, growth dilution caused by a faster growth rate is another contributor to the reduced TMFs in the productive oceans.[24,26] TPSs are not always negatively correlated with primary production. For example, primary production and TPSs are both low in the subtropical oceans with short food-chain lengths (e.g., the South Pacific gyre, the North Atlantic gyre near Africa, and the South Atlantic gyre near South America). These regions with super low productivity cannot support much biomass.[62] Additionally, the TMFs are low in these regions. An observation found that short food chains result in low Hg biomagnification in the tropical Western Africa.[30]

In the high-latitude oceans (e.g., the Arctic Ocean and the Southern Ocean adjacent to Antarctica), despite the high TPSs, the TMFs are not high (Figures 2 and 3). In contrast, Lavoie et al.[26] found significant biomagnification in the cold high-latitude systems due to the low growth rate (i.e., no growth dilution) and low excretion rate. Our previous findings suggest that the excretion rate has weak effects on the MMHg biomagnification in plankton systems.[24] The absence of high-trophic-level predators (Figure 4) may explain the low modeled TMFs in these regions.[30] The short food chain of producers to copepods was observed in the high-latitude Scotia Sea.[63]

Diversity and primary production show high spatial correlation (Figures S3 and S5). Diversity is maximum in mid-productivity regions and saturates where the primary production is considerably high (Figure S6a). Al-Reasi et al. found that the complex species' diversity in the tropical marine ecosystems leads to the lower Hg biomagnification.[64] Our model results show that generally high diversity reduces MMHg biomagnification in the low- and mid-latitude oceans. However, the diversity and TMFs are not strongly correlated (Figure S6b) as the TPS is more closely related to productivity than diversity in spatial patterns.

3.3. Future Scenarios. In the future ocean with the warming climate, reduced rates of nutrient supply will lower the primary production in low latitudes,[18] but in the high-latitude oceans, increased growth rates due to increased temperatures lead to higher productivity (Figure S3b), which is consistent with previous modeling studies.[19] The changes in the modeled diversity are relatively large but without a strong spatial coherence (Figure S5b). With a lower primary production, the TPSs are increased in the low- and mid-latitude oceans (Figure 3b). The trophic positions in the future are similar to those of today, indicating that, at least within the model, the food-chain length will not change much (Figure 1). This is probably because there is no population extinction or outbreak in the simulated future and the fraction of a certain prey in a predator's diet composition will not change a lot.

The average MMHg concentrations in the low-trophic-level plankton barely change. Experimental studies show the similar results that MMHg uptake by the phytoplankton is not sensitive to changes in temperature.[27] However, MMHg concentrations in the plankton at high TLs (>3) are increased considerably, leading to more significant biomagnification (Figure 1b), consistent with field data.[65−67] Consumers will exert a greater predation pressure on the plankton at lower TLs to meet their rising energy demands in warmer environments[20] (Figure S8). Grazing (and photosynthesis) in the ecosystem model are parameterized following an Arrhenius curve such that they increase exponentially with temperature.[32] Also, the higher temperature accelerates the bioconcentration (k_{BC} in eq 2); thus, more MMHg is taken up by the zooplankton, especially for the larger zooplankton. With lower productivity, the decline of biomass with TLs becomes weaker in the future (Figure 3b). A more significant MMHg biomagnification on a larger scale is predicted in the future as the oligotrophic waters are expanding with global warming.[68] Although it is debatable whether warming will promote the energy transfer in the food web,[21] an observation in a subtropical lake does confirm that the biomagnification of persistent pollutants such as polycyclic hydrocarbons is enhanced with the high temperature in planktonic food webs.[65] Additionally, for high-trophic-level organisms such as fish, both model and field data show that rising temperatures lead to increases in MMHg concentrations, suggesting more human exposure to MMHg through seafood in the warming future.[66]

https://doi.org/10.1021/acs.est.1c04083
Environ. Sci. Technol. XXXX, XXX, XXX−XXX

■ ASSOCIATED CONTENT

Supporting Information

The Supporting Information is available free of charge at https://pubs.acs.org/doi/10.1021/acs.est.1c04083.

Parameters for the model; observed TMFs in the marine plankton; schematic of the modeled marine plankton food webs; spatial pattern of the plankton, primary production, ratio of the zooplankton to phytoplankton biomass, and diversity; relationships between diversity, primary production, and TMFs; relationships between biomass and TLs; and changes in grazing fluxes in the future (PDF)

■ AUTHOR INFORMATION

Corresponding Author

Yanxu Zhang − *School of Atmospheric Sciences, Nanjing University, Nanjing, Jiangsu 210023, China;* orcid.org/0000-0001-7770-3466; Email: zhangyx@nju.edu.cn

Authors

Peipei Wu − *School of Atmospheric Sciences, Nanjing University, Nanjing, Jiangsu 210023, China*

Stephanie Dutkiewicz − *Department of Earth, Atmospheric, and Planetary Sciences and Center for Climate Change Science, Massachusetts Institute of Technology, Cambridge, Massachusetts 02139, United States*

Erwan Monier − *Department of Land, Air and Water Resources, University of California, Davis, Davis, California 95616, United States*

Complete contact information is available at: https://pubs.acs.org/10.1021/acs.est.1c04083

Notes

The authors declare no competing financial interest.

■ ACKNOWLEDGMENTS

The authors gratefully acknowledge the financial support from the National Natural Science Foundation of China (grant nos. 41875148 and 42177349), the Fundamental Research Funds for the Central Universities (grant no. 020714380168), the Frontiers Science Center for Critical Earth Material Cycling, Jiangsu Innovation and Entrepreneurial Talents Plan, and the Collaborative Innovation Center of Climate Change, Jiangsu Province. We are grateful to the High Performance Computing Center of Nanjing University for doing the numerical calculations in this paper on its blade cluster system.

■ REFERENCES

(1) Budnik, L. T.; Casteleyn, L. Mercury pollution in modern times and its socio-medical consequences. *Sci. Total Environ.* **2019**, *654*, 720−734.

(2) Axelrad, D. A.; Bellinger, D. C.; Ryan, L. M.; Woodruff, T. J. Dose-response relationship of prenatal mercury exposure and IQ: An integrative analysis of epidemiologic data. *Environ. Health Perspect.* **2007**, *115*, 609−615.

(3) Sakamoto, M.; Tatsuta, N.; Izumo, K.; Phan, P.; Vu, L.; Yamamoto, M.; Nakamura, M.; Nakai, K.; Murata, K. Health impacts and biomarkers of prenatal exposure to methylmercury: Lessons from Minamata, Japan. *Toxics* **2018**, *6*, 45.

(4) FAO. *FAO Yearbook of Fishery and Aquaculture Statistics*, 2017.

(5) Sunderland, E. M.; Li, M.; Bullard, K. Erratum: "Decadal Changes in the Edible Supply of Seafood and Methylmercury Exposure in the United States". *Environ. Health Perspect.* **2018**, *126*, 029003.

(6) Višnjevec, A. M.; Kocman, D.; Horvat, M. Human mercury exposure and effects in Europe. *Environ. Toxicol. Chem.* **2014**, *33*, 1259−1270.

(7) Zhang, Y.; Song, Z.; Huang, S.; Zhang, P.; Peng, Y.; Wu, P.; Gu, J.; Dutkiewicz, S.; Zhang, H.; Wu, S.; Wang, F.; Chen, L.; Wang, S.; Li, P. Global Health Effects of Future Atmospheric Mercury Emissions. *Nat. Commun.* **2021**, *12*, 3035.

(8) Trudel, M.; Rasmussen, J. B. Modeling the elimination of mercury by fish. *Environ. Sci. Technol.* **1997**, *31*, 1716−1722.

(9) Chasar, L. C.; Scudder, B. C.; Stewart, A. R.; Bell, A. H.; Aiken, G. R. Mercury cycling in stream ecosystems. 3. Trophic dynamics and methylmercury bioaccumulation. *Environ. Sci. Technol.* **2009**, *43*, 2733−2739.

(10) Hill, W. R.; Stewart, A. J.; Napolitano, G. E. Mercury speciation and bioaccumulation in lotic primary producers and primary consumers. *Can. J. Fish. Aquat. Sci.* **1996**, *53*, 812−819.

(11) Stewart, A. R.; Saiki, M. K.; Kuwabara, J. S.; Alpers, C. N.; Marvin-Dipasquale, M.; Krabbenhoft, D. P. Influence of plankton mercury dynamics and trophic pathways on mercury concentrations of top predator fish of a mining-impacted reservoir. *Can. J. Fish. Aquat. Sci.* **2008**, *65*, 2351−2366.

(12) Gasol, J. M.; del Giorgio, P. A.; Duarte, C. M. Biomass distribution in marine planktonic communities. *Limnol. Oceanogr.* **1997**, *42*, 1353−1363.

(13) Calbet, A. Mesozooplankton grazing effect on primary production: A global comparative analysis in marine ecosystems. *Limnol. Oceanogr.* **2001**, *46*, 1824−1830.

(14) Hatton, I. A.; McCann, K. S.; Fryxell, J. M.; Davies, T. J.; Smerlak, M.; Sinclair, A. R. E.; Loreau, M. The predator-prey power law: Biomass scaling across terrestrial and aquatic biomes. *Science* **2015**, *349*, aac6284.

(15) Armengol, L.; Calbet, A.; Franchy, G.; Rodríguez-Santos, A.; Hernández-León, S. Planktonic food web structure and trophic transfer efficiency along a productivity gradient in the tropical and subtropical Atlantic Ocean. *Sci. Rep.* **2019**, *9*, 2044.

(16) Irigoien, X.; Huisman, J.; Harris, R. P. Global biodiversity patterns of marine phytoplankton and zooplankton. *Nature* **2004**, *429*, 863−867.

(17) Vallina, S.; Follows, M.; Dutkiewicz, S.; Montoya, J.; Cermeno, P.; Loreau, M. Global relationship between phytoplankton diversity and productivity in the ocean. *Nat. Commun.* **2014**, *5*, 4299.

(18) Dutkiewicz, S.; Scott, J. R.; Follows, M. J. Winners and losers: Ecological and biogeochemical changes in a warming ocean. *Global Biogeochem. Cycles* **2013**, *27*, 463−477.

(19) Lewandowska, A. M.; Boyce, D. G.; Hofmann, M.; Matthiessen, B.; Sommer, U.; Worm, B. Effects of sea surface warming on marine plankton. *Ecol. Lett.* **2014**, *17*, 614.

(20) O'Gorman, E. J.; Petchey, O. L.; Faulkner, K. J.; Gallo, B.; Gordon, T. A. C.; Neto-Cerejeira, J.; Ólafsson, J. S.; Pichler, D. E.; Thompson, M. S. A.; Woodward, G. A simple model predicts how warming simplifies wild food webs. *Nat. Clim. Change* **2019**, *9*, 611−616.

(21) Barneche, D. R.; Hulatt, C. J.; Dossena, M.; Padfield, D.; Woodward, G.; Trimmer, M. Gabriel Yvon-Durocher Warming impairs trophic transfer efficiency in a long-term field experiment. *Nature* **2021**, *592*, 76−79.

(22) Alvain, S.; Moulin, C.; Dandonneau, Y.; Loisel, H. Seasonal distribution and succession of dominant phytoplankton groups in the global ocean: A satellite view. *Global Biogeochem. Cycles* **2008**, *22*, GB3001.

(23) Barton, A. D.; Dutkiewicz, S.; Flierl, G.; Bragg, J.; Follows, M. J. Patterns of diversity in marine phytoplankton. *Science* **2010**, *327*, 1509−1511.

(24) Wu, P.; Zakem, E. J.; Dutkiewicz, S.; Zhang, Y. Biomagnification of methylmercury in a marine plankton ecosystem. *Environ. Sci. Technol.* **2020**, *54*, 5446−5455.

(25) Jędruch, A.; Beldowska, M.; Ziółkowska, M. The role of benthic macrofauna in the trophic transfer of mercury in a low-diversity temperate coastal ecosystem (Puck Lagoon, southern Baltic Sea). *Environ. Monit. Assess.* **2019**, *191*, 137.
(26) Lavoie, R. A.; Jardine, T. D.; Chumchal, M. M.; Kidd, K. A.; Campbell, L. M. Biomagnification of mercury in aquatic food webs: A worldwide meta-analysis. *Environ. Sci. Technol.* **2013**, *47*, 13385−13394.
(27) Schartup, A. T.; Qureshi, A.; Dassuncao, C.; Thackray, C. P.; Harding, G.; Sunderland, E. M. A model for methylmercury uptake and trophic transfer by marine plankton. *Environ. Sci. Technol.* **2018**, *52*, 654−662.
(28) Chen, C. Y.; Folt, C. L. High plankton densities reduce mercury biomagnification. *Environ. Sci. Technol.* **2005**, *39*, 115−121.
(29) Chouvelon, T.; Cresson, P.; Bouchoucha, M.; Brach-Papa, C.; Bustamante, P.; Crochet, S.; Marco-Miralles, F.; Thomas, B.; Knoery, J. Oligotrophy as a major driver of mercury bioaccumulation in medium-to high-trophic level consumers: A marine ecosystem-comparative study. *Environ. Pollut.* **2018**, *233*, 844−854.
(30) Ouédraogo, O.; Chételat, J.; Amyot, M. Bioaccumulation and Trophic Transfer of Mercury and Selenium in African Sub-Tropical Fluvial Reservoirs Food Webs (Burkina Faso). *PLoS One* **2015**, *10*, No. e0123048.
(31) Zhang, Y.; Soerensen, A. L.; Schartup, A. T.; Sunderland, E. M. A global model for methylmercury formation and uptake at the base of marine food web. *Global Biogeochem. Cycles* **2020**, *34*, No. e2019GB006348.
(32) Dutkiewicz, S.; Cermeno, P.; Jahn, O.; Follows, M. J.; Hickman, A. E.; Taniguchi, D. A. A.; Ward, B. A. Dimensions of marine phytoplankton diversity. *Biogeosciences* **2020**, *17*, 609−634.
(33) Dutkiewicz, S.; Sokolov, A.; Scott, J.; Stone, P. A Three-Dimensional Ocean-Seaice-Carbon Cycle Model and its Coupling to a Two-Dimensional Atmospheric Model: Uses in Climate Change Studies. *122. Joint Program on the Science and Policy of Global Change*, 2005.
(34) Monier, E.; Paltsev, S.; Sokolov, A.; Chen, Y.-H. H.; Gao, X.; Ejaz, Q.; Couzo, E.; Schlosser, C. A.; Dutkiewicz, S.; Fant, C.; Scott, J.; Kicklighter, D.; Morris, J.; Jacoby, H.; Prinn, R.; Haigh, M. Toward a consistent modeling framework to assess multi-sectoral climate impacts. *Nat. Commun.* **2018**, *9*, 660.
(35) Zhang, Y.; Jacob, D. J.; Dutkiewicz, S.; Amos, H. M.; Long, M. S.; Sunderland, E. M. Biogeochemical drivers of the fate of riverine mercury discharged to the global and Arctic oceans. *Global Biogeochem. Cycles* **2015**, *29*, 854−864.
(36) Large, W. G.; Mcwilliams, J. C.; Doney, S. C. Oceanic vertical mixing: A review and a model with a nonlocal boundary layer parameterization. *Rev. Geophys.* **1994**, *32*, 363−403.
(37) Gent, P. R.; Mcwilliams, J. C. Isopycnal mixing in ocean circulation models. *J. Phys. Oceanogr.* **1990**, *20*, 150−155.
(38) Monier, E.; Scott, J. R.; Sokolov, A. P.; Forest, C. E.; Schlosser, C. A. An integrated assessment modeling framework for uncertainty studies in global and regional climate change: the MIT IGSM-CAM (version 1.0). *Geosci. Model Dev.* **2013**, *6*, 2063−2085.
(39) Moss, R. H.; Edmonds, J. A.; Hibbard, K. A.; Manning, M. R.; Rose, S. K.; van Vuuren, D. P.; Carter, T. R.; Emori, S.; Kainuma, M.; Kram, T.; Meehl, G. A.; Mitchell, J. F. B.; Nakicenovic, N.; Riahi, K.; Smith, S. J.; Stouffer, R. J.; Thomson, A. M.; Weyant, J. P.; Wilbanks, T. J. The next generation of scenarios for climate change research and assessment. *Nature* **2010**, *463*, 747−756.
(40) Jeong, H. J.; Yoo, Y. D.; Kim, J. S.; Seong, K. A.; Kang, N. S.; Kim, T. H. Growth, feeding and ecological roles of the mixotrophic and heterotrophic dinoflagellates in marine planktonic food webs. *Ocean Sci. J.* **2010**, *45*, 65−91.
(41) Hansell, D.; Carlson, C.; Repeta, D.; Schlitzer, R. Dissolved Organic Matter in the Ocean: A Controversy Stimulates New Insights. *Oceanography* **2009**, *22*, 202−211.
(42) Horowitz, H. M.; Jacob, D. J.; Zhang, Y.; Dibble, T. S.; Slemr, F.; Amos, H. M.; Schmidt, J. A.; Corbitt, E. S.; Marais, E. A.; Sunderland, E. M. A new mechanism for atmospheric mercury redox chemistry: Implications for the global mercury budget. *Atmos. Chem. Phys.* **2017**, *17*, 6353−6371.
(43) Pauly, D.; Trites, A. W.; Capuli, E.; Christensen, V. Diet composition and trophic levels of marine mammals. *ICES J. Mar. Sci.* **1998**, *55*, 467−481.
(44) Borgå, K.; Kidd, K. A.; Muir, D. C.; Berglund, O.; Conder, J. M.; Gobas, F. A.; Kucklick, J.; Malm, O.; Powell, D. E. Trophic magnification factors: Considerations of ecology, ecosystems, and study design. *Integr. Environ. Assess. Manage.* **2012**, *8*, 64−84.
(45) Romanuk, T. N.; Hayward, A.; Hutchings, J. A. Trophic level scales positively with body size in fishes. *Global Ecol. Biogeogr.* **2010**, *20*, 231−240.
(46) Gosnell, K. J.; Mason, P. R. Mercury and methylmercury incidence and bioaccumulation in plankton from the central Pacific Ocean. *Mar. Chem.* **2015**, *177*, 772−780.
(47) Lee, C.-S.; Fisher, N. S. Methylmercury uptake by diverse marine phytoplankton. *Limnol. Oceanogr.* **2016**, *61*, 1626−1639.
(48) Hirota, R.; Fukuda, Y.; Chiba, J.; Tajima, S.; Fujiki, M. Mercury content of copepods (*Crustacea*) collected from the Antarctic Sea. *Polar Res. Repos.* **1989**, *2*, 65−70.
(49) Trebilco, R.; Baum, J. K.; Salomon, N. K. Ecosystem ecology: size-based constraints on the pyramids of life. *Trends Ecol. Evol.* **2013**, *28*, 423−431.
(50) Ward, D. M.; Nislow, K. H.; Folt, C. L. Bioaccumulation syndrome: identifying factors that make some stream food webs prone to elevated mercury bioaccumulation. *Ann. N.Y. Acad. Sci.* **2010**, *1195*, 62−83.
(51) Kehrig, H. A.; Palermo, E. F. A.; Seixas, T. G.; Branco, C. W. C.; Moreira, I.; Malm, O. Trophic transfer of methylmercury and trace elements by tropical estuarine seston and plankton. *Estuar. Coast Shelf Sci.* **2009**, *85*, 36−44.
(52) Lavoie, R. A.; Hebert, C. E.; Rail, J.-F.; Braune, B. M.; Yumvihoze, E.; Hill, L. G.; Lean, D. R. S. Trophic structure and mercury distribution in a Gulf of St. Lawrence (Canada) food web using stable isotope analysis. *Sci. Total Environ.* **2010**, *408*, 5529−5539.
(53) Loseto, L. L.; Stern, G. A.; Deibel, D.; Connelly, T. L.; Prokopowicz, A.; Lean, D. R. S.; Fortier, L.; Ferguson, S. H. Linking mercury exposure to habitat and feeding behaviour in Beaufort Sea beluga whales. *J. Mar. Syst.* **2008**, *74*, 1012−1024.
(54) Hammerschmidt, C. R.; Finiguerra, M. B.; Weller, R. L.; Fitzgerald, W. F. Methylmercury accumulation in plankton on the continental margin of the Northwest Atlantic Ocean. *Environ. Sci. Technol.* **2013**, *47*, 3671−3677.
(55) Hammerschmidt, C. R.; Fitzgerald, W. F. Bioaccumulation and trophic transfer of Methylmercury in Long Island Sound. *Arch. Environ. Contam. Toxicol.* **2006**, *51*, 416−424.
(56) Fox, A. L.; Trefry, J. H.; Trocine, R. P.; Dunton, K. H.; Lasorsa, B. K.; Konar, B.; Ashjian, C. J.; Cooper, L. W. Mercury biomagnification in food webs of the northeastern Chukchi Sea, Alaskan Arctic. *Deep Sea Res., Part II* **2017**, *144*, 63−77.
(57) Campbell, L. M.; Norstrom, R. J.; Hobson, K. A.; Muir, D. C. G.; Backus, S.; Fisk, A. T. Mercury and other trace elements in a pelagic Arctic marine food web (Northwater Polynya, Baffin Bay). *Sci. Total Environ.* **2005**, *351−352*, 247−263.
(58) Di Beneditto, A. P. M.; Bittar, V. T.; Camargo, P. B.; Kehrig, H. A. Mercury and nitrogen isotope in a marine species from a tropical coastal food web. *Arch. Environ. Contam. Toxicol.* **2012**, *62*, 264−271.
(59) Thera, J. C.; Rumbold, D. G. Biomagnification of mercury through a subtropical coastal food web off Southwest Florida. *Environ. Toxicol. Chem.* **2013**, *33*, 65−73.
(60) Liu, J.; Cao, L.; Dou, S. Trophic transfer, biomagnification and risk assessments of four common heavy metals in the food web of Laizhou Bay, the Bohai Sea. *Sci. Total Environ.* **2019**, *670*, 508−522.
(61) Ward, B. A.; Dutkiewicz, S.; Follows, M. J. Modelling spatial and temporal patterns in size-structured marine plankton communities: top−down and bottom−up controls. *J. Plankton Res.* **2013**, *36*, 31−47.

https://doi.org/10.1021/acs.est.1c04083
Environ. Sci. Technol. XXXX, XXX, XXX−XXX

(62) Morel, A.; Claustre, H.; Gentili, B. The most oligotrophic subtropical zones of the global ocean: similarities and differences in terms of chlorophyll and yellow substance. *Biogeosciences* **2010**, *7*, 3139−3151.
(63) Stowasser, G.; Atkinson, A.; McGill, R. A. R.; Phillips, R. A.; Collins, M. A.; Pond, D. W. Food web dynamics in the Scotia Sea in summer: A stable isotope study. *Deep Sea Res., Part II* **2012**, *59*−*60*, 208−221.
(64) Al-Reasi, H. A.; Ababneh, F. A.; Lean, D. R. Evaluating mercury biomagnification in fish from a tropical marine environment using stable isotopes (δ13C AND δ15N). *Environ. Toxicol. Chem.* **2010**, *26*, 1572−1581.
(65) Tao, Y.; Xue, B.; Lei, G.; Liu, F.; Wang, Z. Effects of climate change on bioaccumulation and biomagnification of polycyclic aromatic hydrocarbons in the planktonic food web of a subtropical shallow eutrophic lake in China. *Environ. Pollut.* **2017**, *223*, 624−634.
(66) Schartup, A. T.; Thackray, C. P.; Qureshi, A.; Dassuncao, C.; Gillespie, K.; Hanke, A.; Sunderland, E. M. Climate change and overfishing increase neurotoxicant in marine predators. *Nature* **2019**, *572*, 648−650.
(67) Wu, P.; Kainz, M. J.; Valdés, F.; Zheng, S.; Winter, K.; Wang, R.; Branfireun, B.; Chen, C. Y.; Bishop, K. Elevated temperature and browning increase dietary methylmercury, but decrease essential fatty acids at the base of lake food webs. *Sci. Rep.* **2021**, *11*, 16859.
(68) Polovina, J. J.; Howell, E. A.; Abecassis, M. Ocean's least productive waters are expanding. *Geophys. Res. Lett.* **2008**, *35*, L03618.

https://doi.org/10.1021/acs.est.1c04083
Environ. Sci. Technol. XXXX, XXX, XXX−XXX